

Stability and tolerance to impurities of the fluorinated surface of hydrogen-absorbing alloys

X.-L. Wang, S. Suda

Department of Chemical Engineering, Kogakuin University, 2665-1 Nakano-machi, Hachioji-shi, Tokyo 192, Japan

Received 27 October 1994; in final form 3 March 1995

Abstract

The surface structure of a fluorinated $\text{LaNi}_{4.7}\text{Al}_{0.3}$ alloy that was ground by hydriding–dehydriding (H–D) cycling was determined by means of scanning electron microscopy, electron probe microanalysis and X-ray photoelectron spectroscopy. The change and the stability of the fluorinated surface were studied after exposure to water and air for various periods, and after further H–D cycles. It was found that an LaF_3 layer was formed on the surfaces of the particles and on the surfaces of the cracks that were formed during H–D cycling, after treating the sample with an F^- -containing aqueous solution. Excellent hydriding characteristics were observed for the fluorinated alloy. After exposure of the fluorinated sample to air and water for a long period, and after repeating the reaction cycles with pure hydrogen gas or H_2 gas containing CO, a stable LaF_3 layer still remained on the surface. Excellent reactivity was still maintained, correspondingly. The degradation of the hydriding reaction rate and of the hydrogen capacity of the fluorinated alloy were found to be very small, even when using a $\text{H}_2 + 300$ ppm CO gas mixture at lower temperatures. On the contrary, this gas mixture deactivates the untreated alloy severely under the same conditions. These observations indicate that the overlying fluoride layer can effectively protect the sublayer from impurities.

Keywords: Hydrogen absorbing alloys; Metal hydrides; Surface treatment; Fluorination

1. Introduction

In recent years, metal hydrides (MH) have been applied for developing energy conversion devices such as electric and thermal energy storage units, heat pumps, hydrogen purification–separation and rechargeable batteries [1]. Steady reaction and long durability are required for those applications while the required properties are strongly dependent on the surface structures and compositions.

One of the possibly successful application of hydrogen-absorbing alloys is thought to be the hydrogen purification and separation. The characteristics of the purification and separation will depend significantly on, among other things, the sensitivity of the metal surface which will be damaged by various non- H_2 impurities in the hydrogen. In addition, in many applications hydrogen-absorbing alloys are likely to be exposed to air for a long period in practical situations. In this case, surface passivation resulting from the surface oxidation and contamination during air exposure occurs and made the initial activation difficult. The longer the alloys are exposed to air after crushing, the more difficult the initial activation becomes.

In practical applications, hydrogen-absorbing alloys will be pulverized during hydriding–dehydriding (H–D) cycles.

This pulverization causes a substantial increase in fresh surfaces, segregations and microcracks and promotes pyrophoricity and surface poisoning. This surface damage has markedly limited the applications of hydrogen-absorbing alloys for hydrogen separation and purification.

These difficulties in initial activation and high sensitivity to gaseous impurities have been pointed out as two of the five major shortcomings in MH applications [2].

To overcome those difficulties, a new surface treatment method has been developed by employing an F^- -containing aqueous solution [3] and applied to several kinds of alloys, the AB, AB_2 , A_2B and AB_5 -type alloys. The surface compositions and structures of the fluorinated alloys have been revealed [4]. For typical AB_5 -type alloys, e.g. $\text{LaNi}_{4.7}\text{Al}_{0.3}$, the surface structure after F treatment showed that LaF_3 had formed on the top surface which was followed by an Ni-rich sub-layer. The F treatment greatly improved the gaseous hydriding properties and the initial activation characteristics [5]. It is also recognized that the surface treatment can provide an excellent effect for protecting the surface contaminations by poisonous materials such as air, water vapor, carbon monoxide and carbon dioxide. These new surface structures formed by the F treatment encouraged practical applications of hydrogen-absorbing alloys in many areas. It

is also expected that, in practical commercial applications, the benefits of F treatment persist even after storage for a long period in air and water or after repeating many H–D reaction cycles.

This investigation is devoted to revealing the surface structures and compositions of the H–D ground and then fluorinated fine powder alloys. It also aims at examining the change in surface structure and the stability of fluoride layer after exposing the fluorinated alloy to water and air for various periods, especially after performing further H–D cycles. Subsequently, the tolerance to impurities of the fluorinated surface will be examined, and the relationship of surface structure and reaction characteristics will be correlated. In [6–8] it was found that CO seriously poisons the AB₅-type alloys at lower temperatures (lower than 100 °C). Therefore the gas mixture, H₂ + 300 ppm CO, was selected in this work as an extreme poisoning source in order to examine the tolerance of the fluorinated surface to impurities.

In this investigation, both electron probe microanalysis (EMPA) and X-ray photoelectron spectroscopy (XPS) were used to analyze the surface structure and composition. The sample selected as a typical AB₅-type alloy was LaNi_{4.7}Al_{0.3}.

2. Experimental details

An LaNi_{4.7}Al_{0.3} alloy produced by vacuum induction melting process was supplied by Japan Metals & Chemical Ltd. Co. The sample was ground to a fine powder (with numerous cracks) by repeating several H–D cycles and then treated in an F[−]-containing aqueous solution at room temperature, keeping a constant weight-to-volume ratio of the powder samples to the treatment solution. The fluorinated samples were rinsed several times with tap water and dried in air.

The fluorinated samples were separated into three parts: the first part was exposed to water and the second part was exposed to air. These two samples were investigated after storage for 3, 15 and 30 days. For the third sample, a further 15 H–D cycles were performed, then it was exposed to air.

Analyses of the surface morphology and the composition of those samples were carried out using an electron probe microanalyzer (Shimadzu EPMA-8705), a scanning electron microscopy attached to the microanalyser and an X-ray photoelectron spectrometer (Shimadzu ESCA-850M). The particles were mounted in a special resin and polished with diamond oil slurry (0.1 μm) in the final step to determine the composition profiles across sections of particles.

In the determination of the tolerance to impurity exposure of the fluorinated surface, experiments were carried out using a Sievert-type apparatus. 15 g of the fluorinated sample were used. The temperature was set as 333.2 K and the initial pressure was set at 1.5 MPa for each H–D cycle, the mixed gas being H₂ + 300 ppm CO. Changes in the pressure were measured using a data acquisition system (Hewlett–Packard 3052A) with an electric pressure transducer (model PLC) at 0.2 s intervals.

3. Results and discussion

3.1. Surface structures of the fluorinated and untreated alloys

The morphology of the H–D ground and then fluorinated LaNi_{4.7}Al_{0.3} was viewed by SEM. Fig. 1 illustrates the scanning electron micrographs of the untreated and fluorinated surfaces. It was observed that the untreated alloy had been pulverized to an average size of 30 μm (by considering cracks, the real size was about 5 μm), and numerous cracks were formed after repeating the H–D cycles. The width of the large cracks reached about 1 μm and the surface was very smooth. After treatment with an F[−]-containing aqueous solution, very fine crystallites were observed on the surface.

Composition profiles across the sections of particles were determined by EMPA. Fig. 2 shows the characteristic X-ray images where these X-ray images are negative for clear observation, i.e. darker areas indicate increased elemental concentration. As the distributions of the elements La, Ni and Al



(a)



(b)

Fig. 1. SEM images revealing the surface morphology of the H–D ground LaNi_{4.7}Al_{0.3} particles (a) before and (b) after F treatment.

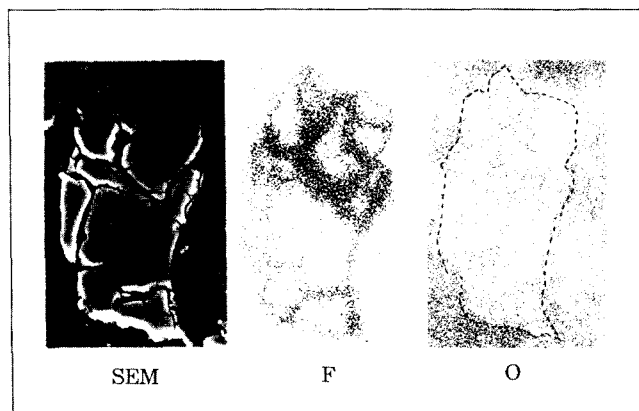


Fig. 2. SEM images and elemental X-ray images of sectional particles for the fluorinated $\text{LaNi}_{4.7}\text{Al}_{0.3}$.

were observed to be homogeneous, Fig. 2 only reveals the presence of the elements F and O. It is clearly seen from these images that F is distributed homogeneously on the outer surface and on the surfaces of cracks. However, it is very hard to observe oxygen on the surfaces. This implies that the oxide or hydroxide on the initial surfaces was removed during F treatment and an overlying fluoride layer had formed on the surfaces of the particles and also the surfaces of cracks. The top layer of a few micrometers thickness was confirmed to be LaF_3 , which accompanies the Ni-rich sublayer phases. These results have been reported elsewhere [4].

3.2. Stability of the fluorinated surface after exposure to air, water and after further hydriding–dehydriding cycles

3.2.1. After exposure to air and water

The morphology of the samples exposed to water and air for various periods was examined by SEM. It was revealed that the morphology of the surface could not be markedly changed.

Composition profiles across the sections of particles were determined by EPMA. Fig. 3 shows the characteristic X-ray

images for the sectional surfaces of the alloys exposed to water and air for 15 days. It can be seen that the elemental distributions were homogeneous and that the fluoride still remained on the surface. Oxygen was hard to observe on the surface. Samples exposed for other periods showed similar results. EPMA analyses indicate that the elemental distribution did not markedly change even after a long-time exposure. Further examinations were performed by analyzing the changes of chemical state for each element by means of XPS.

The elements La, Ni, Al, O, F of the alloys exposed to air and water for different periods were analyzed. It was observed that Ni was maintained as metallic. A change in the F 1s core level was not observed. This implies that the LaF_3 remained stably on the surface regardless of exposure period to both air and water, and this can effectively protect the subsurface.

Regarding the change in oxygen, a small splitting in the O 1s core level was observed (532 eV and 530 eV) after exposure for longer than 15 days to air and 30 days to water [9]. By exposing the sample to water, the splitting of the O 1s core level appeared much later than that by exposing the sample to air. This indicates that no heavy hydroxidation occurred during exposure to water and the surface was much more stable than during exposure to air. The smallness of the O 1s core level splitting in both exposures indicates that no heavy oxidation or hydroxidation occurred. A quantitative analysis of the change in oxygen was performed. Fig. 4 shows the comparison of three different samples, i.e. the samples exposed to water and air, and the sample without F treatment (hand crushed). The ratio of the oxygen content on the fresh surface (before exposure) to the oxygen content on the surface after exposure for various periods was plotted as a function of exposure time. It can be seen that there was almost no oxygen increase up to 30 days exposure to water. The increase in oxygen on the surface of particles exposed to air was also very small. However, the surface was heavily oxidized for the samples without F treatment. When comparing these changes, it can be concluded that the overlying fluoride layer is stable regardless of the storage method and time and hence

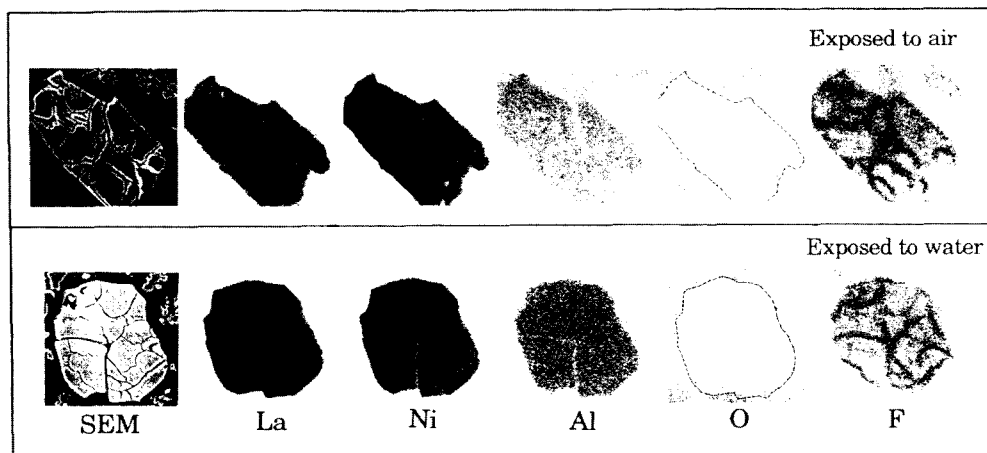


Fig. 3. Elemental X-ray images of sectional particles of the fluorinated $\text{LaNi}_{4.7}\text{Al}_{0.3}$, which was exposed to air (upper part) and water (lower part) for 15 days.

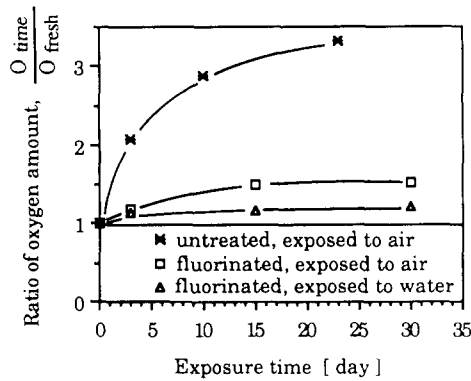


Fig. 4. The comparison of the change in oxygen amount on the surface after exposure to water and air for various periods; O_{fresh} is the oxygen amount on the surface before exposure and O_{time} is the oxygen amount on the surface after exposure for various periods.

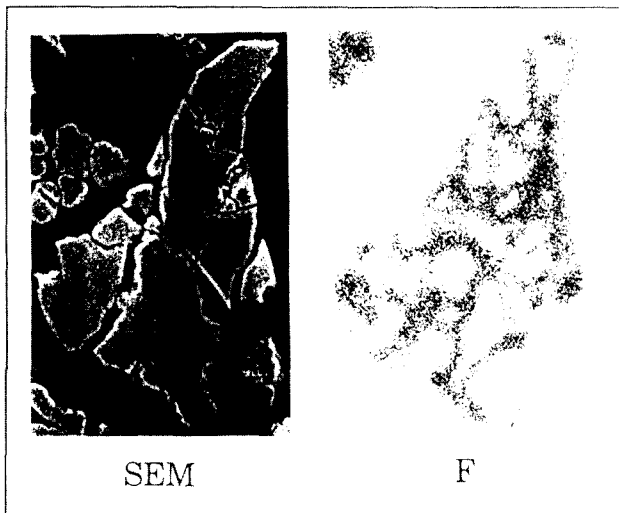


Fig. 5. SEM images and elemental X-ray images of sectional particles for the fluorinated $\text{LaNi}_{4.7}\text{Al}_{0.3}$ after further H–D cycles.

can effectively protect the sublayer from impurities such as oxygen and water.

3.2.2. After further hydriding–dehydriding

After H–D grinding and subsequent F treatment, the fluorinated particles were further cycled with hydrogen gas by repeating 15 H–D cycles and then exposed to air in order to determine the change of surface structure, the stability of the fluoride layer and the protective characteristics of the fluorinated surface from impurities. By means of EPMA, the composition profiles across the sections of particles were determined. Fig. 5 shows the results obtained from a relatively small particle (no new surfaces were formed during H–D cycling). It can be seen that the fluoride layer on the surfaces of the particles and also the surfaces of cracks still remained. This implies that the fluoride layer could not be removed by repeating H–D cycles and by heating or evacuating the samples.

Further determinations were performed on initially larger particles where some new microcracks were formed during H–D cycles. Fig. 6 illustrates the characteristic X-ray images across the sections of particles. It is clearly seen from these images that the LaF_3 layer on most of the surfaces still present even after repeating many H–D cycles. However, no fluoride layer was observed on some parts of the surfaces and cracks. This implies that those surfaces and cracks were freshly formed during H–D cycles. When comparing the amount of oxygen on the freshly formed surface with that on the LaF_3 -covered surface, it was observed that the amount of oxygen on the freshly formed surface was much larger than that on the LaF_3 -covered surface. These observations revealed that the overlying fluoride layer can effectively protect the sublayer from impurities.

3.3. Tolerance of the fluorinated surface to air, water and CO

It has been found through the above observations that the overlying fluoride layer formed during F treatment can remain stable on the surface after exposing to both air and water for a long period, and even after repeating many H–D cycles. By utilizing these characteristics, experiments were

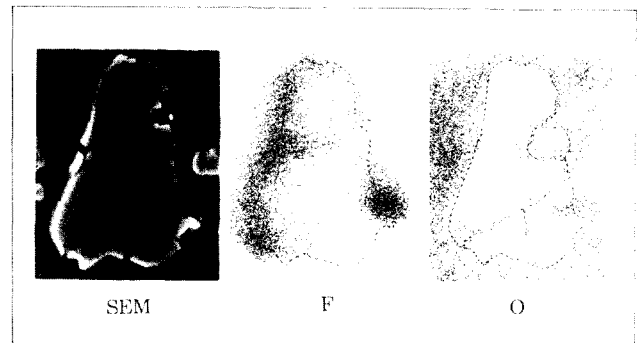


Fig. 6. Illustration of the oxidation at the fluorinated surfaces after further H–D cycles.

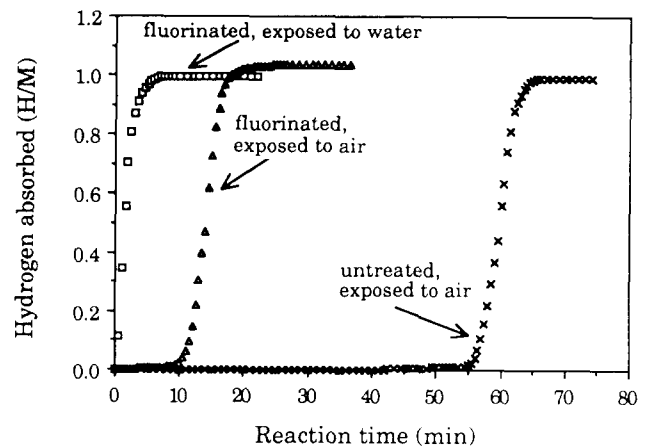


Fig. 7. Comparison of the initial activation for the untreated and fluorinated $\text{LaNi}_{4.7}\text{Al}_{0.3}$ after exposure to air and water for 60 days; the data were taken at 313.2 K under an initial hydrogen pressure of 1.0 MPa.

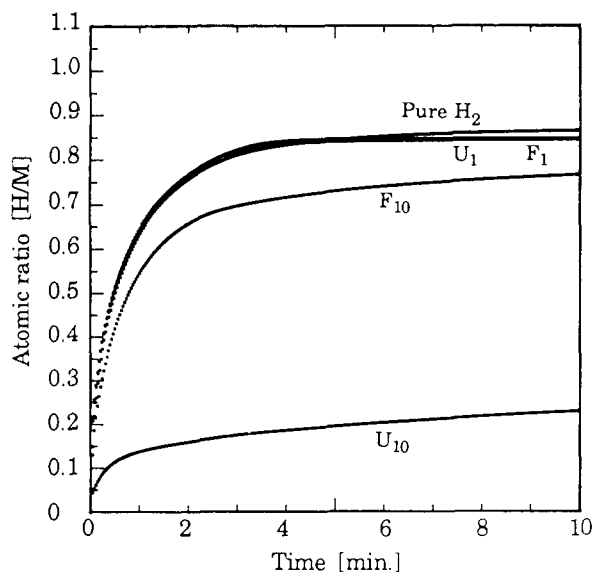


Fig. 8. The change of hydriding reaction rate as a function of cyclic number for the untreated and fluorinated $\text{LaNi}_{4.7}\text{Al}_{0.3}$ at 333.2 K using a mixed gas $\text{H}_2 + 300$ ppm: curve U_1 , untreated, the first cycle using the mixed gas; curve F_1 fluorinated, the first cycle using the mixed gas; curve U_{10} , untreated, the tenth cycle using the mixed gas; curve F_{10} , fluorinated, the tenth cycle using the mixed gas.

performed to determine the initial activation properties after exposing to air and water, and the tolerance to impurities under various conditions. Fig. 7 shows the comparison of the initial activation rates for both the untreated and fluorinated samples which were exposed to water and air for 60 days [10]. It was observed that the incubation time for the untreated sample was about 55 min after 60 days exposure to air because of the surface contamination, i.e. surface oxidation and hydroxidation. However, the fluorinated sample exposed under the same conditions showed a much shorter incubation time (only 10 min). In particular, for the water-exposed sample, no incubation was observed even after exposure for 60 days. These observations revealed that the excellent reactivity was still maintained and the F treatment can provide an excellent means for protecting from surface contamination by poisonous materials such as air and water. These reaction results are in concord with the results of the surface analysis obtained by EPMA and XPS.

A further examination was devoted to the effects of the extremely poisonous impurity CO on the hydriding reactions. Fig. 8 shows the effects of CO on the hydriding reaction rates for the fluorinated alloy where the data were obtained at 333.2 K using the mixed gas ($\text{H}_2 + 300$ ppm CO). For comparison, the results obtained from the untreated sample under the same conditions are shown in the same figure. We observed that the reaction rate rapidly decreased with increasing number of reaction cycles for the untreated sample. At the tenth cycle, the amount of hydrogen absorbed after 10 min was only about 24% of that when using pure hydrogen. However, after surface treatment, the degradation of the hydriding reaction rate

and the hydrogen capacity were found to be quite small when CO was present. It is clear that the fluorinated surface shows an impressive tolerance to CO poisoning.

On the basis of the above observations, it can be concluded that an excellent reactivity of the fluorinated alloys can be maintained even after fairly long exposure to water and air or after cyclic H–D reactions in the presence of a damaging gas such as CO. Furthermore, the unique surface structure where LaF_3 was formed on the surface on top of an Ni-rich sublayer can be kept stable regardless of storage method, storage period, H–D cycles and existence of impurities. This overlying fluoride layer can effectively protect the sublayer from impurities while the surface activity is maintained.

4. Conclusions

By surface treatment of an $\text{LaNi}_{4.7}\text{Al}_{0.3}$ alloy with an F^- -containing aqueous solution, an LaF_3 layer was formed on the surfaces of the particles and the surfaces of the cracks that had formed during H–D cycling. Metallic Ni was precipitated in a sublayer below the LaF_3 layer. Excellent hydriding reaction rates were obtained. The overlying fluoride layer can effectively protect the sublayer from impurities even for the extremely poisonous CO. It can remain stable on the surface of particles even after many H–D cycles or after a long-time exposure to water and air. The stable and protective surface effects can offer the first real hope towards practical hydride-based applications such as hydrogen separation and purification from gas mixtures involving damaging gases such as CO, O_2 , H_2O or others because the principal problem for hydrogen separation and purification is the extreme surface damage by gaseous impurities.

Acknowledgments

The authors wish to thank N. Haraikawa, T. Ebihara and K. Iwata for experimental assistance.

References

- [1] G.D. Sandrock and S. Suda, Applications, in L. Schlapbach (ed.), *Hydrogen in Intermetallic Compounds II, Top. Appl. Phys.*, 67 (1992).
- [2] S. Suda and G.D. Sandrock, *Z. Phys. Chem.*, 183 (1994) 149.
- [3] S. Suda, *Jpn. Kokai Tokkyo Koho JP 05 213 601*, 19 .
- [4] X.-L. Wang and S. Suda, *J. Alloys Comp.*, 194 (1993) 73.
- [5] F.-J. Liu, G. Sandrock and S. Suda, *J. Alloys Comp.*, 192 (1992) 57.
- [6] G.D. Sandrock and P.D. Goodell, *J. Less-Common Met.*, 104 (1984) 159.
- [7] P.D. Goodell, *J. Less-Common Met.*, 89 (1983) 45.
- [8] F.G. Eisenberg and P.D. Goodell, *J. Less-Common Met.*, 89 (1983) 55.
- [9] X.-L. Wang, N. Haraikawa and S. Suda, *Trans. Mater. Res. Soc. Jpn. B*, 18 (1994) 1253.
- [10] F.J. Liu, Y. Konishi and S. Suda, *Res. Rep. Kogakuin Univ.*, (74) (1993) 51.